PHYSICAL REVIEW D **87,** 035024 (2013)

Positively deflected anomaly mediation in the light of the Higgs boson discovery

Nobuchika Okada[1,*] and Hieu Minh Tran[2,†]

[1]*Department of Physics and Astronomy, University of Alabama, Tuscaloosa, Alabama 35487, USA*
[2]*Hanoi University of Science and Technology, 1 Dai Co Viet Road, Hanoi, Vietnam*

(Received 18 December 2012; published 21 February 2013)

Anomaly-mediated supersymmetry breaking (AMSB) is a well-known mechanism for flavor-blind transmission of supersymmetry breaking from the hidden sector to the visible sector. However, the pure AMSB scenario suffers from a serious drawback, namely, the tachyonic slepton problem, and needs to be extended. The so-called (positively) deflected AMSB is a simple extension to solve the problem and also provides us with the usual neutralino lightest superpartner as a good candidate for dark matter in the Universe. Motivated by the recent discovery of the Higgs boson at the Large Hadron Collider (LHC) experiments, we perform the parameter scan in the deflected AMSB scenario by taking into account a variety of phenomenological constraints, such as the dark matter relic density and the observed Higgs boson mass around 125–126 GeV. We identify the allowed parameter region and list benchmark mass spectra. We find that in most of the allowed parameter regions, the dark matter neutralino is Higgsino-like and its elastic scattering cross section with nuclei is within the future reach of the direct dark matter search experiments, while (colored) sparticles are quite heavy and their discovery at the LHC is challenging.

DOI: 10.1103/PhysRevD.87.035024 PACS numbers: 12.60.Jv, 95.35.+d, 12.60.−i, 14.80.Ly

I. INTRODUCTION

Recently, the ATLAS [1] and CMS [2] collaborations announced the discovery of a new scalar particle at the Large Hadron Collider (LHC) which is most likely the Standard Model (SM) Higgs boson, with a mass measured, respectively, as

$$m_h = 126.0 \pm 0.4(\text{stat}) \pm 0.4(\text{syst})\ \text{GeV}, \quad (1)$$

$$m_h = 125.3 \pm 0.4(\text{stat}) \pm 0.5(\text{syst})\ \text{GeV}. \quad (2)$$

Although we need more data accumulation to conclude that it is truly the SM Higgs boson, these observations have ignited a new trend of particle physics research. Since the first announcement from CERN about the signal excess in the Higgs boson searches at the LHC, the implication of a 125 GeV Higgs boson has been intensively studied for about a year, in particular the implications for supersymmetric (SUSY) models [3].

SUSY extension of the SM is one of the most promising ways to solve the gauge hierarchy problem, because the quadratic divergences of the Higgs self-energy corrections are completely canceled out by contributions between superpartners and hence SUSY models are insensitive to ultraviolet (UV) physics. Moreover, in the minimal supersymmetric extension of the SM (MSSM) with R-parity conservation, the lightest superpartner (LSP), usually the neutralino, is a weakly interacting massive particle and a good candidate for dark matter in the Universe.

Since none of experiments has directly found superpartners, SUSY must be broken at low energies. In addition, many results of the indirect search for superpartners require a very special way of generating the soft SUSY-breaking terms, namely, they must be almost flavor-blind and CP-invariant. There are several mechanisms that can generate such soft SUSY-breaking terms naturally, such as gauge-mediated SUSY breaking (GMSB) [4] and anomaly-mediated SUSY breaking (AMSB) [5,6].

In this paper, we focus on the AMSB scenario where SUSY breaking is mediated to the MSSM sector through the superconformal anomaly. In this scenario, the nonzero vacuum expectation value of the F component of the compensating multiplet (F_ϕ) is the unique SUSY-breaking source that results in all types of soft terms. This scenario is based on supergravity and hence AMSB contributions to soft terms always exist. In the usual supergravity scenario, F_ϕ coincides with the gravitino mass, and the gravitino is much heavier than other sparticles in the AMSB scenario (see Ref. [7] for an exception). Unfortunately, the pure AMSB scenario cannot be realistic because the slepton squared masses are predicted to be negative. There are several proposed solutions to this tachyonic slepton problem in the AMSB scenario with simple modifications from the pure AMSB [8–12].

We consider the scenario involving the so-called deflected anomaly mediation [8,11]. The basic idea is to introduce a messenger sector as in the GMSB, and the threshold corrections by the messenger fields deflect the renormalization group (RG) trajectory of the soft terms from those in the pure AMSB scenario. Although this scenario looks similar to the GMSB, there is a crucial difference, namely, the SUSY breaking in the messenger sector is generated by the AMSB and hence the scenario is basically the AMSB scenario. Thus, the SUSY breaking generated in the messenger sector is proportional to the

*okadan@ua.edu
†hieu.tranminh@hust.edu.vn

original SUSY-breaking source: the F-term of the compensating multiplet. The constant of this proportionality is called the "deflection parameter," introduced in Ref. [11], which is a measure of how much the model is deflected from the pure AMSB. Since the SUSY breaking in the messenger sector is secondary, the deflection parameter should be of $\mathcal{O}(1)$, at most, for the sake of theoretical consistency. The deflection parameter can be either negative [8] or positive [11]. Both the resultant sparticle mass spectrum and the cosmological aspects of the scenario are quite different between these two cases. While the LSP was found to be a new particle for a negative deflection parameter [8,13], the deflected AMSB with a positive deflection parameter provides us with the lightest neutralino as the LSP, as is usual in the MSSM [11]. Thus, in this paper we consider the positively deflected AMSB scenario.

The phenomenology of the positively deflected AMSB scenario, especially the dark matter physics, has been previously investigated in Ref. [14]. However, very large values of the deflection parameter $\gg 1$ were taken into account in the previous analysis.[1] Because of the theoretical consistency mentioned above, we constrain the deflection parameter not to exceed $\mathcal{O}(1)$ and reconsider the phenomenology of the positively deflected AMSB scenario. In this paper we perform the parameter scan by taking into account a variety of phenomenological constraints. In particular, the relic abundance of the neutralino dark matter and the observed Higgs boson mass play the crucial roles in identifying the allowed parameter region.

The paper is organized as follows. We give a brief review of the deflected AMSB scenario in Sec. II. In Sec. III, we perform the parameter scan of the positively deflected AMSB scenario by taking into account various phenomenological constraints, and identify the allowed parameter region. We also show the benchmark mass spectra for the parameter sets from the allowed region. For these benchmark points, we calculate the elastic scattering cross section of the dark matter neutralino with nuclei and discuss its implication for future dark matter detection experiments. The last section is devoted to conclusions.

II. DEFLECTED ANOMALY MEDIATION

Assuming the sequestering between the hidden and visible sectors [5], the direct SUSY-breaking mediation from the hidden sector to the visible one is forbidden. However, it was found that in the context of supergravity, there always exists the SUSY-breaking mediation through the superconformal anomaly, namely, the AMSB [5,6]. In this scenario, sfermion squared masses are predicted to be proportional to the beta-function coefficients of the MSSM gauge coupling RG equations, so that slepton squared masses are negative. In order to solve this tachyonic slepton problem, we introduce the messenger sector similar to that in the minimal GMSB [4]. The corresponding superpotential is given by

$$W = \sum_{i=1}^{N} S\bar{\Psi}_i\Psi^i, \tag{3}$$

where S is a singlet chiral superfield, and N is the number of vectorlike pairs of messengers Ψ^i and $\bar{\Psi}_i$ in the fundamental and antifundamental representations under the MSSM gauge groups. Here we have used the SU(5) gauge group notation for the MSSM gauge group, for simplicity, under which the messengers are the vectorlike pairs of the $\mathbf{5} + \mathbf{5}^*$ representation.

Once the nonzero vacuum expectation values of the scalar and F-components of S are developed, the messenger sector gives rise to the GMSB-like contributions to the soft SUSY-breaking terms, which can be represented as

$$\frac{F_S}{S} = dF_\phi, \tag{4}$$

where the coefficient d is the deflection parameter. In the deflected anomaly mediation, F_S is generated by the primary SUSY-breaking source F_ϕ. In a simple scenario, the deflection parameter is evaluated as [11]

$$d \sim -2\frac{\frac{\partial W}{\partial S}}{S\frac{\partial^2 W}{\partial S^2}} \tag{5}$$

from the superpotential of the singlet superfield $W(S)$. Since this SUSY breaking in the messenger sector is a secondary SUSY breaking, the theoretical consistency requires $|d| \lesssim \mathcal{O}(1)$; in other words, the secondary SUSY-breaking order parameter cannot be much greater than the primary SUSY-breaking scale F_ϕ.

By using the method established in Ref. [16], the soft SUSY-breaking terms can be extracted from the renormalized gauge couplings and the supersymmetric wave-function renormalization coefficients as follows [8,11]:

$$\frac{M_i(\mu)}{\alpha_i(\mu)} = \frac{F_\phi}{2}\left(\frac{\partial}{\partial \ln \mu} - d\frac{\partial}{\partial \ln |S|}\right)\frac{1}{\alpha_i(\mu, S)}, \tag{6}$$

$$m_I^2(\mu) = -\frac{|F_\phi|^2}{4}\left(\frac{\partial}{\partial \ln \mu} - d\frac{\partial}{\partial \ln |S|}\right)^2 \ln Z_I(\mu, S), \tag{7}$$

$$A_I(\mu) = -\frac{F_\phi}{2}\left(\frac{\partial}{\partial \ln \mu} - d\frac{\partial}{\partial \ln |S|}\right)\ln Z_I(\mu, S), \tag{8}$$

where the gauge couplings and the wave-function renormalization coefficients are given by

[1] In this case, the particle mass spectrum is similar to the one in the GMSB, but with a heavy gravitino. For a theoretically consistent and natural realization of such a mass spectrum as well as neutralino dark matter physics in the setup, see Ref. [15].

$$\alpha_i^{-1}(\mu, S) = \alpha_i^{-1}(\Lambda_{\rm cut}) + \frac{b_i - N}{4\pi} \ln \frac{S^\dagger S}{\Lambda_{\rm cut}^2} + \frac{b_i}{4\pi} \ln \frac{\mu^2}{S^\dagger S}, \tag{9}$$

$$Z_I(\mu, S) = \sum_{i=1,2,3} Z_I(\Lambda_{\rm cut}) \left(\frac{\alpha(\Lambda_{\rm cut})}{\alpha(S)}\right)^{\frac{2c_i}{b_i - N}} \left(\frac{\alpha(S)}{\alpha(\mu)}\right)^{\frac{2c_i}{b_i}}. \tag{10}$$

The index $i = 1, 2, 3$ corresponds to the MSSM gauge group $\mathrm{U}(1)_Y \times \mathrm{SU}(2)_L \times \mathrm{SU}(3)_C$, and $b_i = \{-33/5, -1, 3\}$ $(i = 1, 2, 3)$ are the beta-function coefficients of the MSSM gauge coupling RG equations. The messenger scale $M_{\rm Mess} = S$ plays the role of the intermediate threshold between the UV cutoff $\Lambda_{\rm cut}$ and the electroweak scale.

Substituting Eqs. (9) and (10) into Eqs. (6) and (7), we obtain the solutions for the RG equations of the soft terms. At the messenger scale, the MSSM gaugino masses are given by

$$M_i(M_{\rm Mess}) = -\frac{\alpha_i}{4\pi} F_\phi (b_i + dN). \tag{11}$$

For the A parameters of the third generation, we have

$$A_t(M_{\rm Mess}) = -\frac{F_\phi}{(4\pi)^2}\left(6|Y_t|^2 + |Y_b|^2 - \frac{16}{3}g_3^2 - 3g_2^2 - \frac{13}{15}g_1^2\right), \tag{12}$$

$$A_b(M_{\rm Mess}) = -\frac{F_\phi}{(4\pi)^2}\left(|Y_t|^2 + 6|Y_b|^2 + |Y_\tau|^2 - \frac{16}{3}g_3^2 - 3g_2^2 - \frac{18}{5}g_1^2\right), \tag{13}$$

$$A_\tau(M_{\rm Mess}) = -\frac{F_\phi}{(4\pi)^2}\left(3|Y_b|^2 + 4|Y_\tau|^2 - 3g_2^2 - \frac{9}{5}g_1^2\right), \tag{14}$$

where $Y_{t,b,\tau}$ are the Yukawa couplings of the third-generation quarks and lepton. Finally, the sfermion squared masses are given by

$$m_{H_u}^2(M_{\rm Mess}) = m_{H_d}^2(M_{\rm Mess}) = F_\phi^2\left[\frac{3}{10}\left(\frac{\alpha_1}{4\pi}\right)^2 G_1 + \frac{3}{2}\left(\frac{\alpha_2}{4\pi}\right)^2 G_2\right], \tag{15}$$

$$m_{\tilde{L}}^2(M_{\rm Mess}) = F_\phi^2\left[\frac{3}{10}\left(\frac{\alpha_1}{4\pi}\right)^2 G_1 + \frac{3}{2}\left(\frac{\alpha_2}{4\pi}\right)^2 G_2\right], \tag{16}$$

$$m_{\tilde{E}}^2(M_{\rm Mess}) = F_\phi^2\left[\frac{6}{5}\left(\frac{\alpha_1}{4\pi}\right)^2 G_1\right], \tag{17}$$

$$m_{\tilde{Q}}^2(M_{\rm Mess}) = F_\phi^2\left[\frac{1}{30}\left(\frac{\alpha_1}{4\pi}\right)^2 G_1 + \frac{3}{2}\left(\frac{\alpha_2}{4\pi}\right)^2 G_2 + \frac{8}{3}\left(\frac{\alpha_3}{4\pi}\right)^2 G_3\right], \tag{18}$$

$$m_{\tilde{U}}^2(M_{\rm Mess}) = F_\phi^2\left[\frac{8}{15}\left(\frac{\alpha_1}{4\pi}\right)^2 G_1 + \frac{8}{3}\left(\frac{\alpha_3}{4\pi}\right)^2 G_3\right], \tag{19}$$

$$m_{\tilde{D}}^2(M_{\rm Mess}) = F_\phi^2\left[\frac{2}{15}\left(\frac{\alpha_1}{4\pi}\right)^2 G_1 + \frac{8}{3}\left(\frac{\alpha_3}{4\pi}\right)^2 G_3\right], \tag{20}$$

where

$$G_i = Nd^2 + 2Nd + b_i. \tag{21}$$

These soft terms are used as the boundary conditions for the RG-equation evolution of MSSM soft terms in our analysis. Note that the limit $d = 0$ reproduces the pure AMSB result for the soft terms, while the limits $d \to \infty$ and $F_\phi \to 0$ (while keeping dF_ϕ finite) leads to the soft terms in the GMSB scenario.

III. NUMERICAL ANALYSIS

In the deflected AMSB scenario, the soft terms are characterized by five free parameters,

$$N, d, M_{\rm Mess}, F_\phi, \tan\beta, \tag{22}$$

and one sign of the μ parameter. In this paper, we only consider $\mathrm{sign}(\mu) = +$, which gives rise to a positive contribution of sparticles to the muon anomalous magnetic moment. For various fixed values of N, d, and $\tan\beta$, we scan over the other free parameters $M_{\rm Mess}$ and F_ϕ and identify a parameter region which is consistent with a variety of phenomenological constraints. For numerical analysis, we employ the SOFTSUSY package version 3.3.1 [17] to solve the MSSM RG equations and compute the mass spectrum, with the inputs of the gaugino masses, A parameters, and the sfermion squared masses at the messenger scale given in the previous section. The MICROMEGAS package version 2.4.5 [18] is used to calculate the neutralino dark matter relic abundance and other phenomenological constraints with the output of SOFTSUSY.

The results are shown in Figs. 1–5. The various values of the resultant SM-like Higgs boson mass are depicted as contours. Since the soft terms at the messenger scale are proportional to F_ϕ, the sparticle masses (except Higgsino masses) scale as F_ϕ. As a result, the SM-like Higgs boson mass, which is mainly controlled by stop masses and A_t, becomes heavier as F_ϕ is raised. For the parameters in the red regions, the relic density of the neutralino dark matter can be consistent with the observed data [19]:

$$\Omega_{\rm CDM} h^2 = 0.1120 \pm 0.0056. \tag{23}$$

Figure 1 shows the results for $N = 1$, $d = 2$, and $\tan\beta = 10$. The region inside the left and right diagonal boundaries is theoretically allowed. In the region outside of the left boundary the LSP is found to be the lighter stau and is excluded due to the electrically charged LSP. Since there appear many dots, the right boundary is not clear compared to the left one. This is because around that region the

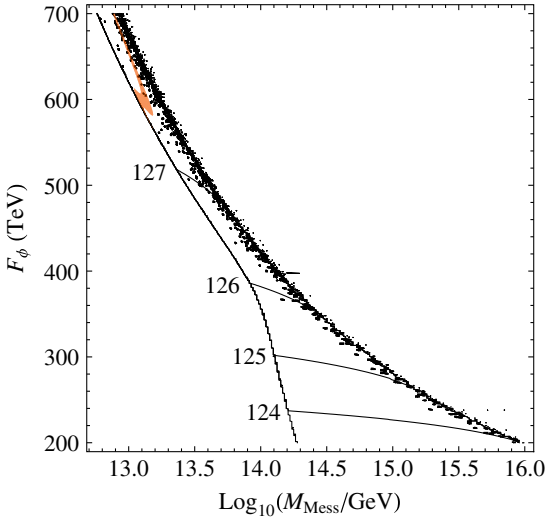

FIG. 1 (color online). Results for $N = 1$, $d=2$, and $\tan\beta=10$. Various values of the resultant SM-like Higgs boson mass are shown as the contours. There are two diagonal boundaries, outside of which values are theoretically excluded. The red strip indicates the region where the relic abundance of neutralino dark matter is consistent with observation.

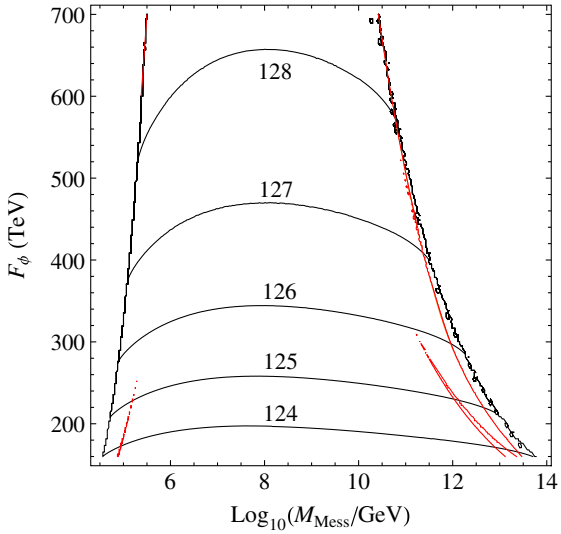

FIG. 3 (color online). Results for $N = 2$, $d=2$, and $\tan\beta=10$. Various values of the resultant SM-like Higgs boson mass are shown as the contours. There are two diagonal boundaries, outside of which values are theoretically excluded. The four red strips indicate the region where the relic abundance of neutralino dark matter is consistent with observation.

convergence of our numerical analysis with the SOFTSUSY turns out to be very sensitive to the input parameters, and we have omitted the parameter sets which do not converge in the SOFTSUSY analysis. In the region outside of the right boundary, the radiative electroweak symmetry breaking is not achieved (no-EWSB region) and hence the region is excluded.

For $N = 1$ and $d = 2$, we always find $M_2 < M_1$ [see Eq. (11)], and the LSP neutralino will be either wino-like, Higgsino-like, or a mixture of both. In the red region around $F_\phi = 600$ TeV, we have found the wino-like LSP neutralino, while the Higgsino-like neutralino is found along the thin strip for $F_\phi > 600$ TeV. For this region, the Higgs boson mass is predicted as $m_h > 127$ GeV, so that the region reproducing the observed dark matter relic density cannot be compatible with the Higgs boson mass measured by ATLAS and CMS. We have found that this conclusion remains the same for the $N = 1$ case with various values of d and $\tan\beta$.

In Fig. 2, we have examined the case with $N = 2$, $d = 1.5$, and $\tan\beta = 10$. Similarly to Fig. 1, there are two boundaries and the regions outside of them are

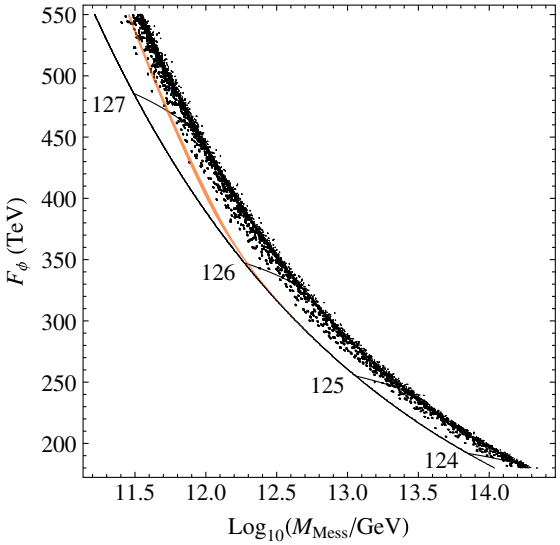

FIG. 2 (color online). The same as in Fig. 1, but for $N = 2$, $d = 1.5$, and $\tan\beta = 10$.

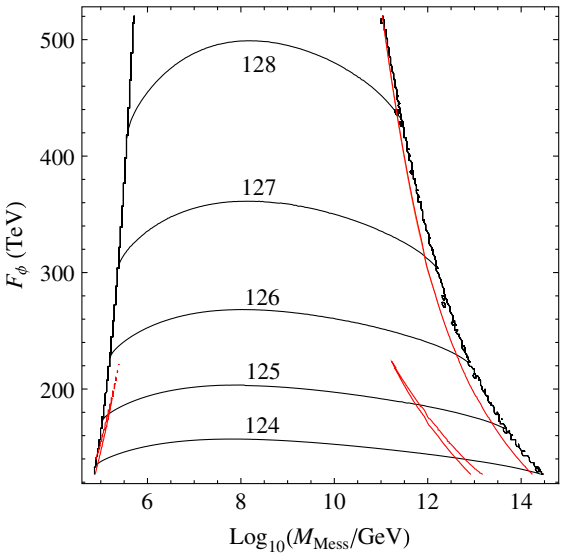

FIG. 4 (color online). The same as in Fig. 3 but for $\tan\beta = 20$.

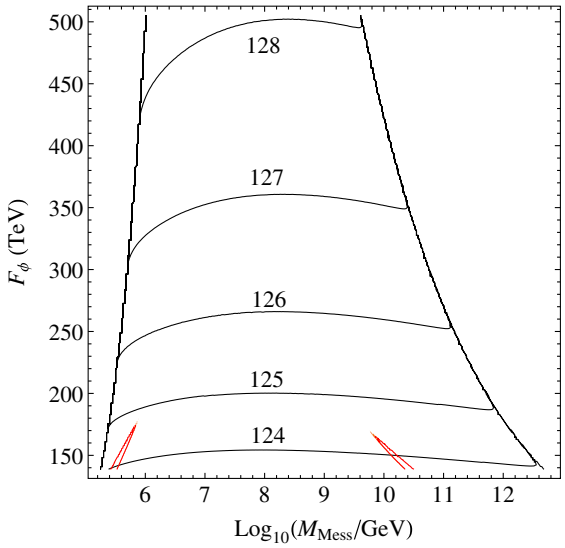

FIG. 5 (color online). The same as in Fig. 3 but for $\tan\beta = 30$.

excluded by the same conditions. Again, the figure shows many dots for the same reason as in Fig. 1. The difference is that in this case the LSP neutralino cannot be wino-like, as can be understood from Eq. (11). We have found that along the thin red strip, the observed dark matter abundance is reproduced with the Higgsino-like LSP neutralino. As F_ϕ becomes larger along the red strip, the LSP neutralino become slightly heavier and the lighter chargino mass becomes closer to the LSP neutralino mass. Note that the parameters on the red strip with 270 TeV $\lesssim F_\phi \lesssim$ 450 TeV predict a Higgs boson mass consistent with the LHC data. When the red region is very close to the left boundary, the lighter stau is very much degenerate with the LSP neutralino. However, the coannihilation process of the LSP neutralino with the stau is not important because its relic abundance is determined dominantly by the neutralino pair annihilation process to $W^\pm$, with the charginos exchanged in the t-channel. Although the sparticle mass spectrum is quite different, the phenomenology of the parameters in the red region is similar to the so-called focus point region in the constrained MSSM, where Higgsino-like neutralinos and charginos are light and the others are quite heavy.

Figure 3 shows the results for $N = 2$, $d = 2$, and $\tan\beta = 10$. Comparing this figure with the previous one, we see a significant movement of the left boundary to the left due to the increase of the deflection parameter $d = 1.5 \to 2$. The conditions that define the left boundary are a little involved. For values of $F_\phi \gtrsim 600$ TeV the left boundary is specified by the no-EWSB condition, while for the parameters outside of the boundary (with $F_\phi \lesssim$ 600 TeV) the CP-odd heavy Higgs boson is found to be tachyonic. The right boundary is specified by the no-EWSB condition as in the previous figures.

The thin red strips show the allowed regions for the relic abundance of the LSP neutralino to be consistent with observation. For parameters on the strip close to the left boundary for $F_\phi \gtrsim 600$ TeV and on the strip along the right boundary, the LSP neutralino is found to be Higgsino-like. As before, this region is similar to the focus point region in the constrained MSSM. On the other red strips, we have found the bino-like neutralino whose mass is close to half of the heavy Higgs boson masses. Thus the correct dark matter abundance is achieved by the s-channel resonance via the heavy Higgs bosons in the neutralino pair annihilation process. These regions correspond to the so-called funnel region in the constrained MSSM. Now we see that three separate regions satisfy the conditions of the dark matter relic abundance and the Higgs boson mass simultaneously, namely, two funnel-like regions and one focus point-like region.

In the following, we keep the values of $N = 2$ and $d = 2$, but raise $\tan\beta$ to 20 and 30. The results are shown in Figs. 4 and 5, respectively. Figure 4 looks identical to Fig. 3 and, in fact, the physics for the allowed regions are the same. However, the left boundary shifts to the right and hence the region inside the two boundaries becomes narrower by the increase of $\tan\beta$. We also see that the funnel-like strips move downward. It can be seen in Fig. 5 that the boundaries shift further (the left boundary shifts to the right and the right boundary shifts to the left) and make the region between them narrower, and the funnel-like strips move further downward. The left boundary in Fig. 5 is specified by the condition of the tachyonic CP-odd Higgs boson, while the right boundary is given by the tachyonic charged Higgs boson, and not by the no-EWSB condition. The red strips along the right boundary in Figs. 3 and 4 disappears in Fig. 5. In this figure, the regions consistent with both the dark matter relic abundance and the Higgs boson mass appear only on the funnel-like strips. When we increase $\tan\beta$ further, we find that the predicted Higgs boson mass in the funnel-like region becomes too small to reproduce the observed Higgs boson mass.

To see the particle mass spectrum, we list four benchmark points in Table I: one from Fig. 2 and the other three from Fig. 3, which simultaneously satisfy the constraints on the neutralino dark matter relic abundance and the measured SM-like Higgs boson mass. In addition to the constraints, we also take into account other phenomenological constraints: the branching ratios of $b \to s\gamma$ [20], $B \to \tau\nu_\tau$ [21], and the muon anomalous magnetic moment $a_\mu = (g_\mu - 2)/2$ [22],

$$2.85 \times 10^{-4} \le \mathrm{BR}(b \to s + \gamma) \le 4.24 \times 10^{-4} (2\sigma), \quad (24)$$

$$\frac{\mathrm{BR}^{\mathrm{exp}}(B \to \tau\nu_\tau)}{\mathrm{BR}^{\mathrm{SM}}(B \to \tau\nu_\tau)} = 1.25 \pm 0.40, \quad (25)$$

$$\Delta a_\mu = a_\mu^{\mathrm{exp}} - a_\mu^{\mathrm{SM}} = (26.1 \pm 8.0) \times 10^{-10} (3.3\sigma). \quad (26)$$

In particular, we consider the most recent limits of the decay process $B_s \to \mu^+\mu^-$ announced by the LHCb Collaboration [23]:

TABLE I. Benchmark particle mass spectra for the case $N = 2$ and $\tan\beta = 10$. Masses of particles are given in GeV. The values of the branching fractions of $b \to s + \gamma$, $B_s \to \mu^+\mu^-$, and $B \to \tau\nu_\tau$, the muon anomalous magnetic dipole moment Δa_μ, and the neutralino relic density are calculated for each benchmark point. The spin-independent and spin-dependent cross sections for the neutralino-proton elastic scattering are also provided.

d	1.5	2	2	2
F_ϕ	2.800×10^5	2.500×10^5	2.500×10^5	2.500×10^5
$M_{\rm Mess}$	6.457×10^{12}	1.902×10^5	6.220×10^{11}	2.176×10^{12}
h^0	125.3	125.3	125.3	125.4
H^0	1389	1850	1921	1595
A^0	1389	1849	1921	1595
$H^\pm$	1391	1851	1923	1597
$\tilde{g}$	10106	10651	10519	10512
$\tilde{\chi}^0_{1,2}$	852.7, 858.5	918.7, 1818	943.2, 1480	900.1, 912.9
$\tilde{\chi}^0_{3,4}$	1422, 1442	1841, 2003	1490, 1918	962.8, 1915
$\tilde{\chi}^\pm_{1,2}$	853.9, 1421	1819, 2003	1480, 1918	913.6, 1914
$\tilde{u}$, $\tilde{c}_{R,L}$	9839, 10200	10522, 10947	10303, 10750	10302, 10748
$\tilde{d}$, $\tilde{s}_{R,L}$	9703, 10200	10494, 10947	10170, 10750	10152, 10748
$\tilde{t}_{1,2}$	7865, 9297	9951, 10670	8377, 9872	8274, 9827
$\tilde{b}_{1,2}$	9296, 9669	10478, 10670	9870, 10137	9826, 10118
$\tilde{\nu}^{e,\mu}_L$	3408	3190	3761	3829
$\tilde{e}$, $\tilde{\mu}_L$	3410, 3408	3191, 3190	3762, 3760	3830, 3828
$\tilde{e}$, $\tilde{\mu}_R$	914.3, 914.1	1284, 1284	1404, 1404	1420, 1420
$\tilde{\nu}^\tau_L$	3400	3188	3754	3821
$\tilde{\tau}_{1,2}$	853.0, 3401	1277, 3189	1368, 3755	1382, 3822
BR$(b \to s + \gamma)$	3.44×10^{-4}	3.38×10^{-4}	3.37×10^{-4}	3.41×10^{-4}
BR$(B_s \to \mu^+\mu^-)$	3.06×10^{-9}	3.06×10^{-9}	3.06×10^{-9}	3.06×10^{-9}
$\frac{\rm BR^{exp}(B\to\tau\nu_\tau)}{\rm BR^{SM}(B\to\tau\nu_\tau)}$	0.997	0.998	0.999	0.998
Δa_μ	3.98×10^{-11}	2.42×10^{-11}	2.38×10^{-11}	2.62×10^{-11}
Ωh^2	0.1121	0.1121	0.1121	0.1121
$\sigma^{\chi-{\rm p}}_{\rm SI}$ (pb)	4.498×10^{-9}	1.426×10^{-11}	8.047×10^{-11}	1.257×10^{-8}
$\sigma^{\chi-{\rm p}}_{\rm SD}$ (pb)	1.325×10^{-6}	2.189×10^{-8}	8.283×10^{-8}	1.025×10^{-5}

$$2.0 \times 10^{-9} < {\rm BR}(B_s \to \mu^+\mu^-) < 4.7 \times 10^{-9} (3.5\sigma). \tag{27}$$

We can see that all the above phenomenological constraints, except for Δa_μ, are well satisfied. The SUSY contribution to the muon anomalous magnetic dipole moment is too small to explain the discrepancy between the observed value and the SM prediction. This is because in order to reproduce the SM-like Higgs boson mass around 125 GeV, the particles are all found to be heavy. This actually happens in most of the well-known SUSY models [3].

In Table I, we see that only the neutralino(s) and chargino can be lighter than 1 TeV. The first column corresponds to a point in Fig. 2, where the LSP neutralino is Higgsino-like. The second and third columns correspond to two points in the funnel-like regions in Fig. 3, where the LSP neutralinos are bino-like. The last column corresponds to a point in Fig. 2, where the LSP neutralino is Higgsino-like, as in the first column.

In Table I, we also list the prediction of the spin-independent (SI) and the spin-dependent (SD) cross sections for neutralino elastic scattering off a proton, which are relevant to the direct/indirect dark matter detection experiments. When the LSP neutralino is bino-like, both the cross sections are very small and beyond the sensitivity of future experiments. On the other hand, for the Higgsino-like neutralino in the first and last columns, we have found $\sigma_{\rm SI} = \mathcal{O}(10^{-8})$ and $\sigma_{\rm SD} = \mathcal{O}(10^{-6}$–$10^{-5})$. Future direct dark matter search experiments, such as XENON1T [24], can cover the SI cross section up to $\sigma_{\rm SI} = \mathcal{O}(10^{-10})$ for a dark matter particle with mass 1 TeV, so that the neutralino dark matter in our scenario can be tested.

IV. CONCLUSIONS

In the positively deflected AMSB, the tachyonic slepton problem in the pure AMSB is ameliorated by introducing the messenger sector that brings the GMSB-like contributions to lift up the slepton squared masses to be positive. In this scenario, the lightest neutralino can be the LSP (as usual) and hence the dark matter candidate. In light of the recent discovery of the Higgs boson at the LHC, we have reconsidered this scenario, in particular the phenomenology

of the neutralino dark matter with natural values of the deflection parameter. We have also taken into account other phenomenological constraints. By fixing N, d, and $\tan\beta$, we have performed the parameter scan with various values of $M_{\rm Mess}$ and F_ϕ and identified the parameter regions that simultaneously satisfy the constraints on the dark matter relic abundance and the observed (SM-like) Higgs boson mass. We have found that in most of the allowed parameter regions, the dark matter neutralino is Higgsino-like. The four benchmark points for the particle spectrum are listed in Table I, for which all phenomenological constraints except the muon anomalous magnetic moment are well satisfied. We have found that although the particle mass spectrum is very high and the SUSY search at the LHC is quite challenging, the SI cross section of the Higgsino-like dark matter stays within the reach of future dark matter direct detection experiments. Thus, such experiments can reveal the signature of SUSY.

Finally, we comment on the following two issues. First, since our resultant sparticle mass spectrum is very high, our scenario needs a fine-tuning for the μ parameter to obtain the correct electroweak scale. For the benchmark points in Table I, we find $\mu \simeq 900$ GeV, so that the level of fine-tuning is about 0.5% when we estimate it by $\frac{m_Z^2}{2\mu^2}$, with m_Z being the Z boson mass. Second, the SM-like Higgs boson can potentially yield deviations in its properties from those of the SM Higgs boson. Although the Higgs boson properties measured at the LHC are mostly consistent with the SM predictions, the signal strength of the diphoton decay mode shows about a 2σ discrepancy between the observed value and the SM expectation [1,2] (see also Refs. [25,26]). This deviation could be an indirect signal of sparticles. For the benchmark points, we have calculated the signal strength for the channel $gg \to h^0 \to \gamma\gamma$ and compared it with the SM prediction. Using the FEYNHIGGS package [27] with the output of SOFTSUSY, we have found that the deviation is about a few percent, and hence negligible. This is also because of the heavy sparticle mass spectrum.

ACKNOWLEDGMENTS

The work of N. O. is supported in part by the DOE Grant No. DE-FG02-10ER41714. H. M. T. would like to thank The Theoretical Group, University of Lyon 1 (especially Aldo Deandrea) for hospitality and the LIA-FVPPL project for financial support during his visit.

[1] The ATLAS Collaboration, Phys. Lett. B **716**, 1 (2012).
[2] The CMS Collaboration, Phys. Lett. B **716**, 30 (2012).
[3] See, for example, I. Gogoladze, Q. Shafi, and C. S. Un, J. High Energy Phys. 08 (2012) 028; A. Arbey, M. Battaglia, A. Djouadi, F. Mahmoudi, and J. Quevillon, Phys. Lett. B **708**, 162 (2012); P. Draper, P. Meade, M. Reece, and D. Shih, Phys. Rev. D **85**, 095007 (2012); M. Carena, S. Gori, N. R. Shah, and C. E. M. Wagner, J. High Energy Phys. 03 (2012) 014; M. Kadastik, K. Kannike, A. Racioppi, and M. Raidal, J. High Energy Phys. 05 (2012) 061; U. Ellwanger, J. High Energy Phys. 03 (2012) 044; S. Akula, B. Altunkaynak, D. Feldman, P. Nath, and G. Peim, Phys. Rev. D **85**, 075001 (2012); K. Cheung and T.-C. Yuan, Phys. Rev. Lett. **108**, 141602 (2012); J. F. Gunion, Y. Jiang, and S. Kraml, Phys. Lett. B **710**, 454 (2012); J. L. Evans, M. Ibe, S. Shirai, and T. T. Yanagida, Phys. Rev. D **85**, 095004 (2012); S. F. King, M. Muhlleitner, and R. Nevzorov, Nucl. Phys. **B860**, 207 (2012); Z. Kang, J. Li, and T. Li, J. High Energy Phys. 11 (2012) 024; L. Aparicio, D. G. Cerdeno, and L. E. Ibanez, J. High Energy Phys. 04 (2012) 126; J. Ellis, K. A. Olive, and K. A. Olive, Eur. Phys. J. C **72**, 2005 (2012); H. Baer, V. Barger, and A. Mustafayev, J. High Energy Phys. 05 (2012) 091; J.-J. Cao, Z.-X. Heng, J. M. Yang, Y.-M. Zhang, and J.-Y. Zhu, J. High Energy Phys. 03 (2012) 086; F. Boudjema and G. D. La Rochelle, Phys. Rev. D **86**, 015018 (2012); D. A. Vasquez, G. Belanger, C. Boehm, J. Da Silva, P. Richardson, and C. Wymant, Phys. Rev. D **86**, 035023 (2012); U. Ellwanger and C. Hugonie, Adv. High Energy Phys. **2012**, 625389 (2012); H. Baer, V. Barger, P. Huang, and X. Tata, J. High Energy Phys. 05 (2012) 109; I. Gogoladze, Q. Shafi, and C. S. Un, J. High Energy Phys. 07 (2012) 055; M. Hindmarsh and D. R. T. Jones, arXiv:1203.6838; M. A. Ajaib, I. Gogoladze, F. Nasir, and Q. Shafi, Phys. Lett. B **713**, 462 (2012); J. L. Evans, M. Ibe, and T. T. Yanagida, Phys. Rev. D **86**, 015017 (2012); T. Basak and S. Mohanty, Phys. Rev. D **86**, 075031 (2012); M. Badziak, E. Dudas, M. Olechowski, and S. Pokorski, J. High Energy Phys. 07 (2012) 155; N. Okada, arXiv:1205.5826; E. Dudas, Y. Mambrini, A. Mustafayev, and K. A. Olive, Eur. Phys. J. C **72**, 2138 (2012); M. Badziak, Mod. Phys. Lett. A **27**, 1230020 (2012); G. Altarelli, arXiv:1206.1476; P. Athron, S. F. King, D. J. Miller, S. Moretti, and R. Nevzorov, Phys. Rev. D **86**, 095003 (2012); A. Arbey, M. Battaglia, A. Djouadi, and F. Mahmoudi, J. High Energy Phys. 09 (2012) 107; E. Hardy, J. March-Russell, and J. Unwin, J. High Energy Phys. 10 (2012) 072; S. Akula, P. Nath, and G. Peim, Phys. Lett. B **717**, 188 (2012); J. Cao, Z. Heng, J. M. Yang, and J. Zhu, J. High Energy Phys. 10 (2012) 079; M. Hirsch, F. R. Joaquim, and A. Vicente, J. High Energy Phys. 11 (2012) 105; K. J. Bae, T. H. Jung, and H. D. Kim, Phys. Rev. D **87**, 015014 (2013); K. Agashe, Y. Cui, and R. Franceschini, arXiv:1209.2115; M. Badziak, S. Krippendorf, H. P. Nilles, and M. W. Winkler, arXiv:1212.0854.
[4] For a general review, see G. F. Giudice and R. Rattazzi, Phys. Rep. **322**, 419 (1999) and references therein.
[5] L. Randall and R. Sundrum, Nucl. Phys. **B557**, 79 (1999).

[6] G. F. Giudice, M. A. Luty, H. Murayama, and R. Rattazzi, J. High Energy Phys. 12 (1998) 027.
[7] M. A. Luty, Phys. Rev. Lett. **89**, 141801 (2002); M. A. Luty and N. Okada, J. High Energy Phys. 04 (2003) 050.
[8] A. Pomarol and R. Rattazzi, J. High Energy Phys. 05 (1999) 013.
[9] E. Katz, Y. Shadmi, and Y. Shirman, J. High Energy Phys. 08 (1999) 015.
[10] I. Jack and D. R. T. Jones, Phys. Lett. B **482**, 167 (2000); N. Arkani-Hamed, D. E. Kaplan, H. Murayama, and Y. Nomura, J. High Energy Phys. 02 (2001) 041.
[11] N. Okada, Phys. Rev. D **65**, 115009 (2002).
[12] R. Sundrum, Phys. Rev. D **71**, 085003 (2005); K. Hsieh and M. A. Luty, J. High Energy Phys. 06 (2007) 062; Y. Cai and M. A. Luty, J. High Energy Phys. 12 (2010) 037; T. Kobayashi, Y. Nakai, and M. Sakai, J. High Energy Phys. 06 (2011) 039.
[13] R. Rattazzi, A. Strumia, and J. D. Wells, Nucl. Phys. **B576**, 3 (2000).
[14] A. Cesarini, F. Fucito, and A. Lionetto, Phys. Rev. D **75**, 025026 (2007).
[15] H.-S. Goh, S.-P. Ng, and N. Okada, J. High Energy Phys. 01 (2006) 147; S.-P. Ng and N. Okada, J. High Energy Phys. 09 (2007) 040.
[16] G. F. Giudice and R. Rattazzi, Nucl. Phys. **B511**, 25 (1998); N. Arkani-Hamed, G. F. Giudice, M. A. Luty, and R. Rattazzi, Phys. Rev. D **58**, 115005 (1998).
[17] B. C. Allanach, Comput. Phys. Commun. **143**, 305 (2002).
[18] G. Belanger, F. Boudjema, A. Pukhov, and A. Semenov, Comput. Phys. Commun. **174**, 577 (2006); **149**, 103 (2002); G. Belanger, F. Boudjema, P. Brun, A. Pukhov, S. Rosier-Lees, P. Salati, and A. Semenov, Comput. Phys. Commun. **182**, 842 (2011).
[19] D. Larson *et al.*, Astrophys. J. Suppl. Ser. **192**, 16 (2011).
[20] Heavy Flavor Averaging Group, arXiv:0704.3575.
[21] O. Buchmueller, R. Cavanaugh, A. De Roeck, J. R. Ellis, H. Flacher, S. Heinemeyer, G. Isidori, K. A. Olive, F. J. Ronga, and G. Weiglein, Eur. Phys. J. C **64**, 391 (2009).
[22] K. Hagiwara, R. Liao, A. D. Martin, D. Nomura, and T. Teubner, J. Phys. G **38**, 085003 (2011).
[23] R. Aaij *et al.* (LHCb Collaboration), Phys. Rev. Lett. **110**, 021801 (2013).
[24] E. Aprile (XENON1T Collaboration), in Proceedings of DM 2012 at UCLA, Los Angeles, CA, 2012 (to be published), arXiv:1206.6288.
[25] The ATLAS Collaboration, Report No. ATLAS-CONF-2012-168.
[26] The CMS Collaboration, Report No. CMS-PAS-HIG-12-015.
[27] S. Heinemeyer, W. Hollik, and G. Weiglein, Comput. Phys. Commun. **124**, 76 (2000); Eur. Phys. J. C **9**, 343 (1999); G. Degrassi, S. Heinemeyer, W. Hollik, P. Slavich, and G. Weiglein, Eur. Phys. J. C **28**, 133 (2003); M. Frank, T. Hahn, S. Heinemeyer, W. Hollik, H. Rzehak, and G. Weiglein, J. High Energy Phys. 02 (2007) 047; S. Heinemeyer, W. Hollik, H. Rzehak, and G. Weiglein, Phys. Lett. B **652**, 300 (2007); T. Hahn, S. Heinemeyer, W. Hollik, H. Rzehak, and G. Weiglein, Comput. Phys. Commun. **180**, 1426 (2009); Nucl. Phys. B, Proc. Suppl. **205–206**, 152 (2010).